AIAA JOURNAL
Vol. 36, No. 9, September 1998

Eigenstructure Assignment Technique for Damage Detection in Rotating Structures

Jason Kiddy* and Darryll Pines†
University of Maryland, College Park, Maryland 20742-3015

The detection and the identification of damage in a helicopter rotor blade are considered. An eigenstructure assignment technique is developed using measured modal test data and a finite element model of the blade to detect and to characterize the extent of damage in the system. Previous eigenstructure assignment techniques have not attempted to consider the centrifugal and gyroscopic forces found in rotating systems. Additional elemental stiffness matrix terms are generated for the inboard elements due to the centrifugal force caused by the mass of the outboard elements. This force creates an enhanced sensitivity of the eigenstructure to mass changes, thereby leading to an improved damage detection capability. The feasibility of the methodology is demonstrated analytically on a finite element model of the TH-55A main rotor blade in a vacuum.

Nomenclature

$[A_{ij}]$	= stiffness influence matrix
a	= damage in stiffness
$[B_{ij}]_k$	= mass influence matrix
b	= damage in mass
$[C]$	= $n \times n$ proportional damping matrix
EI	= structural stiffness
F	= distributed force in z direction
$[F]$	= $n \times p$ control influence matrix
$[G(\Omega)]$	= $n \times n$ skew-symmetric gyroscopic matrix
$[K]$	= $n \times n$ global stiffness matrix
$[M]$	= $n \times n$ global mass matrix
n	= number of degrees of freedom
p	= number of sensors
$[Q_{ij}]$	= combined mass influence matrix
R	= beam radius
$[R_j]$	= jth modal residual
t_b	= thickness of the blade
$\{u\}$	= $p \times 1$ vector of control forces
v	= lag (in-plane) displacement
w	= flap (out-of-plane) displacement
$\{x\}$	= $n \times 1$ displacement vector
$\{\dot{x}\}$	= $n \times 1$ velocity vector
$\{\ddot{x}\}$	= $n \times 1$ acceleration vector
α	= best achievable eigenvector angle
λ_j	= jth eigenvalue
$\{\phi\}$	= mode shape
Ω	= rotation rate
ω	= natural frequency

Subscripts

i	= element number
j	= mode number
x	= lag (in-plane) direction
z	= flap (out-of-plane) direction

Superscripts

achieve	= best achievable eigenvector
CF	= centrifugal
dam	= damaged
NR	= nonrotating
T	= transpose of a matrix
$'$	= rotational degree of freedom
$+$	= pseudoinverse

Received Dec. 11, 1997; revision received May 11, 1998; accepted for publication May 19, 1998.

*Graduate Fellow, Department of Aerospace Engineering. Student Member AIAA.

†Assistant Professor, Department of Aerospace Engineering. Senior Member AIAA.

Introduction

Motivation

THE development of health and usage monitoring systems (HUMS) for rotorcraft has been driven by a desire to reduce the operating costs associated with both civilian and military helicopters. Several recent studies illustrate that the installation of HUMS on civilian or military helicopters may significantly reduce insurance and maintenance costs while improving vehicle reliability and safety.[1,2] The goal of HUMS is to provide real-time information regarding the health of critical flight components.

State of the Art

Health monitoring and damage detection of nonrotating structures using modal test data have received a considerable amount of attention over the past two decades, with a significant increase in the number of published reports appearing in the literature in the last 10 years. The basic idea is that modal parameters, notably frequencies, mode shapes, and modal damping, are a function of the physical properties of the structure (mass, stiffness, damping, and boundary conditions). With this in mind, many researchers have developed several promising modal damage detection methods[3–7] that use damaged eigenvectors and eigenvalues with an initial undamaged model to detect and locate damage in a structure. A comprehensive literature review of these methods is given by Doebling et al.[8]

Application to Rotating Structures

Most of the previously developed modal-based damage detection techniques have been applied to nonrotating structures such as offshore oil platforms, bridges, and trusses. There has been very little work reported in the literature on the detection of damage in rotating structures.[9–14] These structures possess unique characteristics such as centrifugal loading and Coriolis couplings. Thus, their dynamics are quite different from those of nonrotating structures. One of the earliest attempts at determining the effect of damage in rotorcraft flight structures was studied by Azzam and Andrews[9] using simulated math models of the rotor system. Faults were simulated and characterized to help determine their effect on the rotorcraft system response. However, no attempt was made to automate the fault classification process. Following this modeling approach, Ganguli et al.[10] applied finite element analysis to develop comprehensive mathematical models of coupled rotor dynamics to simulate various faults and damaged states in a rotor system. The damaged conditions that were simulated include pitch link failures, moisture absorption,

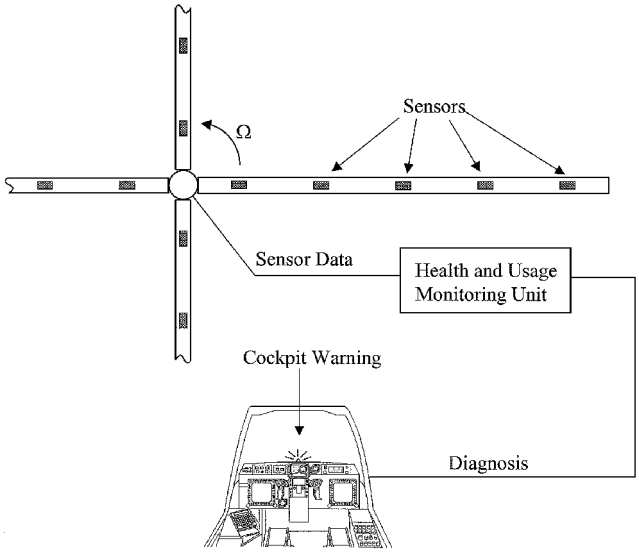

Fig. 1 Real-time main rotor blade health monitoring system.

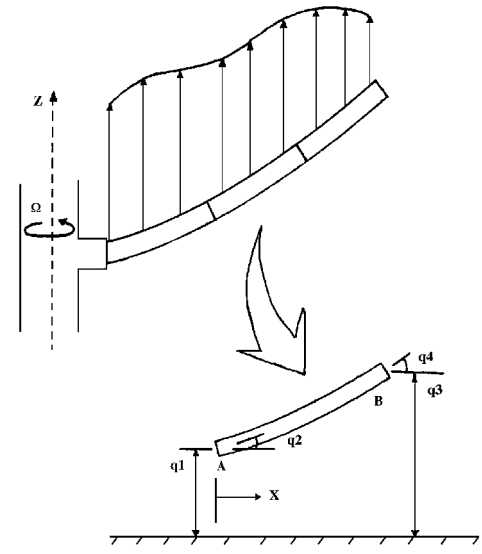

Fig. 2 Finite element model (flap DOF only).

and trim mass loss. The effects of these damaged conditions on rotorcraft system loads were plotted as a function of harmonics of the input rpm. Later, Ganguli et al.[11] trained a neural network to map the input–output response so that damage classification could be performed on the various simulated damage conditions. Although this method has many merits, it is limited to detecting only forms of damage that have been trained by the neural network model. In addition, a large amount of data is required to train the neural network to learn the system model. See Fig. 1 for a picture of a main rotor blade health-monitoring system.

This paper develops an extension to previously developed eigenstructure-assignment-based damage detection methods[7] to account for rotational effects. The extension developed in this paper attempts to account for mass damage that subsequently affects both the system's mass and stiffness matrices due to the centrifugal forces. Previous application of eigenstructure assignment methods to the damage detection problem did not attempt to consider the effect of a mass damage on a structure's stiffness. This paper builds the analytical framework for detecting damage in rotating structures using an eigenstructure assignment methodology. Specifically, damage in rotating helicopter blades is considered as an application of the methodology.

Development of Eigenstructure Assignment Methodology

Model Development

Consider the continuum mechanics description of the coupled flap-lag bending partial differential equations for a rotating beam.[15]

Flap bending:

$$\frac{\mathrm{d}^2}{\mathrm{d}r^2}\left(EI_x\frac{\mathrm{d}^2w}{\mathrm{d}r^2}\right)+m\ddot{w}-\frac{\mathrm{d}}{\mathrm{d}r}\left(\frac{\mathrm{d}w}{\mathrm{d}r}\int_r^R m\Omega^2\rho\,\mathrm{d}\rho\right)+\frac{\mathrm{d}}{\mathrm{d}r}\left(\frac{\mathrm{d}w}{\mathrm{d}r}\int_r^R 2m\Omega\dot{v}\,\mathrm{d}\rho\right)=F_z \tag{1}$$

Lag bending:

$$\frac{\mathrm{d}^2}{\mathrm{d}r^2}\left(EI_z\frac{\mathrm{d}^2v}{\mathrm{d}r^2}\right)+m\ddot{v}-m\Omega^2v-\frac{\mathrm{d}}{\mathrm{d}r}\left(\frac{\mathrm{d}v}{\mathrm{d}r}\int_r^R m\Omega^2\rho\,\mathrm{d}\rho\right)+\frac{\mathrm{d}}{\mathrm{d}r}\left(\frac{\mathrm{d}v}{\mathrm{d}r}\int_r^R 2m\Omega\dot{v}\,\mathrm{d}\rho\right)+2m\Omega\int_0^r\left(\frac{\mathrm{d}v}{\mathrm{d}r}\frac{\mathrm{d}\dot{v}}{\mathrm{d}r}+\frac{\mathrm{d}w}{\mathrm{d}r}\frac{\mathrm{d}\dot{w}}{\mathrm{d}r}\right)\mathrm{d}\rho=F_x \tag{2}$$

A closer inspection of these two equations reveals that the first two terms of each equation are from the standard (nonrotational) Bernoulli–Euler beam equations. The second set of terms, which are proportional to Ω^2, are centrifugal terms, and the remaining terms are due to the Coriolis forces. Note that the Coriolis terms generate gyroscopic coupling between the flap and lag degrees of freedom (DOF) that then affects the overall damping of the system. By linearizing and discretizing the preceding equations into finite elements, one can give the equation of motion for an n-DOF rotating structural system by

$$[M]\{\ddot{x}\}+([C]+[G(\Omega)])\{\dot{x}\}+([K]^{\mathrm{NR}}+[K(\Omega)]^{\mathrm{CF}})\{x\}=[F]\{u\} \tag{3}$$

where $\{x\}=\{w\ \ w'\ \ v\ \ v'\}^T$ is the physical displacement vector.

In the absence of aerodynamic forcing, gyroscopic forces are not present, and by neglecting the proportional damping term due to its small influence on the structural dynamics, the equation of motion can be rewritten as (see Fig. 2)

$$[M]\{\ddot{x}\}+([K]^{\mathrm{NR}}+[K(\Omega)]^{\mathrm{CF}})\{x\}=[F]\{u\} \tag{4}$$

The eigenvalue problem for the rotating blade dynamics can be represented as

$$\left([K]^{\mathrm{NR}}+[K(\Omega)]^{\mathrm{CF}}-\omega_j^2[M]\right)\{\phi\}_j=0 \tag{5}$$

where $\omega_j^2=\lambda_j$.

Damage Approximation

For a damaged blade, we can approximate mass and stiffness damage in terms of a first-order Taylor series expansion given by

$$[M]_{\mathrm{dam}}=[M]+\sum_{i=1}^{N}b_i[M]_i \tag{6}$$

$$[K]_{\mathrm{dam}}=[K]_{\mathrm{dam}}^{\mathrm{NR}}+[K(\Omega)]_{\mathrm{dam}}^{\mathrm{CF_1}}+[K(\Omega)]_{\mathrm{dam}}^{\mathrm{CF_2}} \tag{7}$$

$$[K]_{\mathrm{dam}}^{\mathrm{NR}}=[K]^{\mathrm{NR}}+\sum_{i=1}^{N}a_i[K]_i^{\mathrm{NR}} \tag{8}$$

$$[K(\Omega)]_{\mathrm{dam}}^{\mathrm{CF_1}}=[K]^{\mathrm{CF_1}}+\sum_{i=1}^{N}b_i[K]_i^{\mathrm{CF_1}} \tag{9}$$

$$[K(\Omega)]_{\mathrm{dam}}^{\mathrm{CF_2}}=[K]^{\mathrm{CF_2}}+\sum_{i=1}^{N}\sum_{k=i}^{N}b_k[K]_i^{\mathrm{CF_2}} \tag{10}$$

Note here that the centrifugal portion of the stiffness matrix has been divided into two sections: $[K(\Omega)]^{\mathrm{CF_1}}$, which is affected by a change of mass of a given element (b_i), and $[K(\Omega)]^{\mathrm{CF_2}}$, which

is dependent on both the mass of that element, i, and each of the outboard elements ($b_{k\geq i}$).

Damage Location

Formulating the eigenvalue problem for the damaged structure leads to

$$\left([K]_{\text{dam}} - \lambda_j^{\text{dam}}[M]_{\text{dam}}\right)\{\phi\}_j^{\text{dam}} = 0 \tag{11}$$

Substituting for the first-order approximation to the damaged matrices given in Eqs. (6–10) leads to the following expansion of Eq. (11):

$$\left[[K] + \sum_{i=1}^{N} a_i[K]_i^{\text{NR}} + \sum_{i=1}^{N} b_i[K(\Omega)]_i^{\text{CF}_1} + \sum_{i=1}^{N}\sum_{k=i}^{N} b_k[K(\Omega)]_{ik}^{\text{CF}_2} - \lambda_j^{\text{dam}}\left([M] + \sum_{i=1}^{N} b_i[M]_i\right)\right]\{\phi\}_j^{\text{dam}} = 0 \tag{12}$$

By collecting undamaged and damaged terms, one can rearrange Eq. (12) as

$$\left(\lambda_j^{\text{dam}}[M] - [K]\right)\{\phi\}_j^{\text{dam}} = \sum_{i=1}^{N}\left(a_i[K]_i^{\text{NR}} + b_i[K(\Omega)]_i^{\text{CF}_1} + \sum_{k=i}^{N}\left[b_k[K(\Omega)]_{ik}^{\text{CF}_2}\right] - b_i\lambda_j^{\text{dam}}[M]_i\right)\{\phi\}_j^{\text{dam}} \tag{13}$$

To simplify the preceding expression, define the matrix $[R_j]$ as

$$[R_j] = \left(\lambda_j^{\text{dam}}[M] - [K]\right)^{-1} \tag{14}$$

Now the structural stiffness influence matrix $[A_{ij}]$ and the mass influence matrix $[B_{ij}]_k$ can be defined:

$$[A_{ij}] = [R_j][K]_i^{\text{NR}} \tag{15}$$

$$[B_{ij}]_i = -[R_j][K(\Omega)]_i^{\text{CF}_1} - [R_j][K(\Omega)]_{ii}^{\text{CF}_2} + \lambda_j^{\text{dam}}[R_j][M]_i \tag{16}$$

$$[B_{ij}]_{i+1} = -[R_j][K(\Omega)]_{i(i+1)}^{\text{CF}_2} \tag{17}$$

$$\vdots \qquad \vdots \qquad \vdots$$

$$[B_{ij}]_N = -[R_j][K(\Omega)]_{iN}^{\text{CF}_2} \tag{18}$$

where $[A_{ij}]$ corresponds to the effect of damage associated with the structural stiffness in element i to mode j and $[B_{ij}]_k$ corresponds to damage associated with mass of element k affecting element i and mode j.

By substituting the relations defined in Eqs. (14–18), one can rewrite Eq. (13) as

$$\{\phi\}_j^{\text{dam}} = \sum_{i=1}^{N}([A_{ij}]a_i - [B_{ij}]_i b_i - [B_{ij}]_{i+1}b_{i+1} - \cdots - [B_{ij}]_N b_N)\{\phi\}_j^{\text{dam}} \tag{19}$$

Expanding the summation of Eq. (19) for all elements and collecting terms yields

$$\{\phi\}_j^{\text{dam}} = [A_{1j}]a_1\{\phi\}_j^{\text{dam}} + [A_{2j}]a_2\{\phi\}_j^{\text{dam}} + \cdots + [A_{Nj}]a_N\{\phi\}_j^{\text{dam}} - [B_{1j}]_1 b_1\{\phi\}_j^{\text{dam}} - ([B_{1j}]_2 + [B_{2j}]_2)b_2\{\phi\}_j^{\text{dam}} - \cdots - ([B_{1j}]_N + [B_{2j}]_N + \cdots + [B_{Nj}]_N)b_N\{\phi\}_j^{\text{dam}} \tag{20}$$

For convenience, the matrices can be defined as

$$[Q_{1j}] = -[B_{1j}]_1 \tag{21}$$

$$[Q_{2j}] = -([B_{1j}]_2 + [B_{2j}]_2) \tag{22}$$

$$\vdots \qquad \vdots$$

$$[Q_{Nj}] = -([B_{1j}]_N + [B_{2j}]_N + \cdots + [B_{Nj}]_N) \tag{23}$$

where $[Q_{ij}]$ refers to a mass damage in element i affecting mode j.

Equation (20) can now be written more compactly as

$$\{\phi\}_j^{\text{dam}} = [A_{1j}]a_1\{\phi\}_j^{\text{dam}} + [A_{2j}]a_2\{\phi\}_j^{\text{dam}} + \cdots + [A_{Nj}]a_{Ne}\{\phi\}_j^{\text{dam}} + [Q_{1j}]b_1\{\phi\}_j^{\text{dam}} + [Q_{2j}]b_2\{\phi\}_j^{\text{dam}} + \cdots + [Q_{Nj}]b_N\{\phi\}_j^{\text{dam}} \tag{24}$$

Up to this point, no restrictions have been made as to the number of damaged elements. However, it has been shown that, for simultaneously detecting damage in mass and stiffness matrices, the problem must be constrained to yield a unique solution.[16] If only one element m is considered damaged, i.e., $a_i = b_i = 0$ for $i \neq m$, the necessary constraint is included, and the preceding equation reduces to

$$\{\phi\}_j^{\text{dam}} = [A_{mj}]a_m\{\phi\}_j^{\text{dam}} + [Q_{mj}]b_m\{\phi\}_j^{\text{dam}} \tag{25}$$

This equation can be written in matrix form as

$$[[A_{mj}] \quad [Q_{mj}]]\begin{Bmatrix} a_m\{\phi\}_j^{\text{dam}} \\ b_m\{\phi\}_j^{\text{dam}} \end{Bmatrix} = \{\phi\}_j^{\text{dam}} \tag{26}$$

This equation can be true only if the vector $\{\phi\}_j^{\text{dam}}$ is spanned by the matrix $[L_{mj}] = [[A_{mj}]\ [Q_{mj}]]$. Eigenstructure assignment shows that the eigenvector that best approximates the damaged eigenvector can be obtained from $[L_{mj}]$ and its pseudoinverse leading to[6]

$$\{\phi\}_j^{\text{achieve}} = [L_{mj}]^{+}[L_{mj}]\{\phi\}_j^{\text{dam}} \tag{27}$$

It is now necessary to determine how closely this best achievable eigenvector matches the damaged eigenvector. To do this, the angle between the best achievable eigenvector and the damaged eigenvector can be computed:

$$\alpha = \cos^{-1}\left(\frac{\{\phi\}_j^{\text{achieve}} \cdot \{\phi\}_j^{\text{dam}}}{\left\|\{\phi\}_j^{\text{achieve}}\right\|\left\|\{\phi\}_j^{\text{dam}}\right\|}\right) \tag{28}$$

If the best achievable eigenvector lies parallel to the damaged eigenvector, this angle will be zero. If the angle is not zero, the damaged eigenvector does not lie in the subspace spanned by $[L_{ij}]$, and hence that particular element is not damaged. Through this method, it is possible to determine the damaged element by locating the element i from which $[L_{ij}]$ produces the smallest angle α. Furthermore, the process can be repeated for every mode j. Ideally, α will be zero for the damaged element for every mode.

Extent of Damage

Once the damaged element is determined, the extent of damage in that element can be calculated by rewriting Eq. (26) in a slightly different form:

$$\left[[A_{mj}]\{\phi\}_j^{\text{dam}} \quad [Q_{mj}]\{\phi\}_j^{\text{dam}}\right]\begin{Bmatrix} a_m \\ b_m \end{Bmatrix} = \{\phi\}_j^{\text{dam}} \tag{29}$$

Upon taking the pseudoinverse of the first matrix, we can obtain the extent of damage for a given element as the following:

$$\begin{Bmatrix} a_m \\ b_m \end{Bmatrix} = \left[[A_{mj}]\{\phi\}_j^{\text{dam}} \quad [Q_{mj}]\{\phi\}_j^{\text{dam}}\right]^{+}\{\phi\}_j^{\text{dam}} \tag{30}$$

The accuracy of the preceding damage extent estimate can be improved by using two modes simultaneously in the calculation. Equation (30) is an overdetermined set of equations. The pseudoinverse finds the solution that best solves the equation. By including two

modes in the calculation, the estimate improves. By using the average of various mode combinations, the final estimate of a_m and b_m can be achieved:

$$\begin{Bmatrix} a_m \\ b_m \end{Bmatrix} = \begin{bmatrix} [A_{mj}]\{\phi\}_j^{\text{dam}} & [Q_{mj}]\{\phi\}_j^{\text{dam}} \\ [A_{mk}]\{\phi\}_k^{\text{dam}} & [Q_{mk}]\{\phi\}_k^{\text{dam}} \end{bmatrix}^{+} \begin{Bmatrix} \{\phi\}_j^{\text{dam}} \\ \{\phi\}_k^{\text{dam}} \end{Bmatrix} \tag{31}$$

Modal Expansion

The preceding analysis assumes that all DOF are available to apply the eigenstructure assignment damage detection method. However, the rotational DOF are not easily measured, especially in a rotating environment. For this reason, it is necessary to expand the measured portion of the mode shapes to include all DOF. In this paper, the modal expansion technique developed by Williams and Green[17] is employed to recover the rotational DOF.

Simulation Results

To analytically validate the feasibility of this extension to eigenstructure assignment for damage detection in rotating structures, a detailed finite element model of a scaled rotor blade is considered. To simulate damage, the mass and/or stiffness of one element is reduced. The finite element model is reassembled, and the eigenvalues and eigenvectors of the damaged blade are calculated. These damaged eigenvalues and eigenvectors are used with the undamaged finite element model and the eigenstructure assignment approach to locate and to characterize the damage.

Tables 1 and 2 show the properties of the rotor blade used for this study. These properties correspond to the main rotor blade of a Hughes TH-55A as shown in Figs. 3 and 4. Three different scenarios are considered. The first is the perfect case where all DOF of the finite element model are measured and no noise is present. The second case examines the effect of the modal expansion process on the damage detection algorithm. In this case, only the translational DOF are retained from the eigenvalue analysis of the damaged finite element model. The reduced mode shapes are then expanded to generate the full-DOF mode shapes. The expanded mode shapes are used to characterize the damage. The final scenario is using noisy data with reduced mode shapes. Random noise is simulated on the measured eigenvalues and eigenvectors.

Table 1 Blade reference parameters

Radius, m	1.848
Chord (c/R), m	0.0722
Ω, rad/s	113.8

Table 2 Analytical blade elemental properties

Element	Length, m	Mass, kg	Stiffness, Nm^2
1	0.535	3.467	2999
2	0.610	2.459	2999
3	0.610	2.459	2999
4	0.610	2.459	2999
5	0.610	2.459	2999
6	0.610	3.994	2999

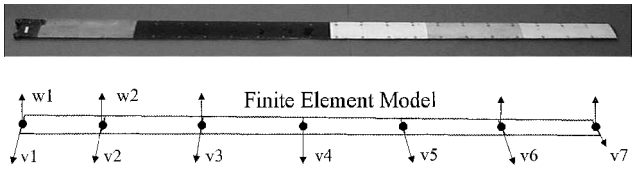

Fig. 3 TH-55A main rotor blade.

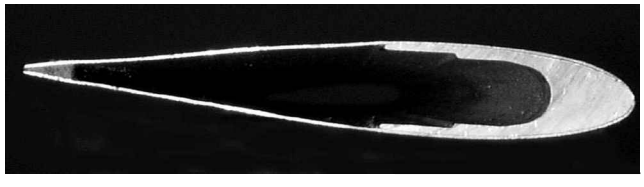

Fig. 4 Cross section of the TH-55A's NACA 0015 airfoil and spar.

For the following examples, the simulated damage is a 10% loss of mass and stiffness in the third of six elements. The first four damaged modes were used to calculate the angle and extent of damage to each element. These modes were used in pairs of two, resulting in six different combinations, i.e., modes 1 and 2, 1 and 3, 1 and 4, 2 and 3, 2 and 4, and 3 and 4. The results were then averaged to arrive at the final results.

Case 1: Fully Populated, Clean Mode Shapes

Nonrotating

Before validating the extension to the eigenstructure assignment methodology on a rotating blade, the method was first tested for a nonrotating blade. In this case, the extension to the eigenstructure assignment condenses into the form given by Lim and Kashangaki.[6] The average values of the angle and extent of damage are shown in Table 3. It can be seen that the location of the damage was properly identified as the third element as it is the only element with $\alpha = 0$. Furthermore, the extent is properly identified by all six combinations of modes.

Rotating

The next test of the methodology is for the same damage case but with the rotational effects included. Again, the mode shapes are fully populated and are not corrupted with noise. The corresponding natural frequencies are listed in Table 4, and the results of the damage detection are included in Table 5. Here it can also be seen that the methodology correctly predicts that $\alpha = 0$ for the third element. The algorithm also properly determines the extent of damage for both mass and stiffness. However, the algorithm determines that $\alpha = 0$ for every element outboard of the third element. This effect is due to the $[Q_{ij}]$ term. For the nonrotating case, $[Q_{ij}]$ simplifies to $[B_{ij}]_i$; $[Q_{ij}]$ contains $[B_{ij}]_i$, but it also contains extra terms due to the centrifugal forces. For higher rotation rates, the centrifugal terms dominate, thereby making $[Q_{ij}]$ for an inboard element linearly dependent on the $[Q_{ij}]$ for every element farther outboard. As the distance from the rotation axis increases, the rank of $[Q_{ij}]$ also increases. Thus, there are more basis vectors to generate the best achievable eigenvector. If an inboard element is able to produce a

Table 3 Damage detection results for 0 rpm and fully populated, clean mode shapes

Element	1	2	3	4	5	6
Average α	0.012	0.012	0.000	0.008	0.011	0.011
Average stiffness change, %	−0.00	−9.69	−10.0	24.6	25.3	21.4
Average mass change, %	−50.2	−7.87	−10.0	23.9	35.4	−0.84

Table 4 Undamaged and damaged natural frequencies

Mode number	Undamaged	Damaged
1	18.6062	18.6060
2	49.5326	50.0518
3	84.0893	84.5939
4	122.0338	122.1325

Table 5 Damage detection results with rotation and fully populated, clean mode shapes

Element	1	2	3	4	5	6
Average angle	0.009	0.003	0.000	0.000	0.000	0.000
Average stiffness change, %	61.9	−125	−10.00	218	55.4	80.2
Average mass change, %	−11.1	−13.2	−10.00	1.89	6.43	2.90

Table 6 Damage detection results with rotation and reduced, clean mode shapes

Element	1	2	3	4	5	6
Average angle	0.009	0.004	0.001	0.000	0.000	0.000
Average stiffness change, %	61.9	−126	−9.06	221	55.4	80.2
Average mass change, %	−11.1	−13.2	−9.96	1.95	6.43	2.91

Table 7 Improved damage location methodology using standard deviations

Element	1	2	3	4	5	6
Stiffness standard deviation	0.6693	2.670	0.020	2.437	1.083	2.037
Mass standard deviation	0.827	0.107	0.000	0.130	0.127	0.032

best achievable eigenvector, then so too are the elements farther outboard for a rotating blade.

For this ideal case, the presence of the additional zero angles does not pose a problem as the element that first shows $\alpha = 0$ denotes the damaged element. However, it will be shown that this is not viable for more realistic situations when the modal data are lacking the rotational DOF or are corrupted with sensor noise.

Case 2: Reduced, Clean Mode Shapes

The third test of the methodology is done by measuring only the translational DOF of the mode shapes. Information about the rotational DOF is recovered using modal expansion. The average results are tabulated in Table 6.

It is shown that the extent of damage in the third element is still predicted at 10% with very little error. However, the angle criteria no longer give a clear indication of which element is damaged. In fact, the angles for elements 4, 5, and 6 are lower than the angle for element 3. Again this is due to the additional rank of the $[Q_{ij}]$ matrix for the outboard elements. Because the angle of the third element is no longer identically zero due to errors in the modal expansion process, the outer elements are able to create a more accurate best achievable eigenvector and hence a lower angle. For this reason, the angle between the best achievable eigenvector and the damaged eigenvector is not a good indicator of the damage location for a rotating system.

To compensate for this problem, a second method of locating damage is developed using a statistical approach. An examination of Eq. (31) shows that it is valid for any combination of two modes (j, k) if the correct element m is assumed to be damaged. Thus, Eq. (31) will yield the same extent of damage regardless of the modes used in the calculation of a_m and b_m. However, this will not be true if the incorrect element is assumed to be damaged. In this case, each combination of modes will provide a different solution to the extent of damage. This fact can be used to provide information on the location of damage. By considering the various combinations of measured modes, the standard deviation can be computed for the extent of damage values (a_m, b_m). Ideally, the damaged element will give a standard deviation of zero. Realistically, the element with the lowest standard deviation represents the damaged element. For the case 2 data just presented, the standard deviations to the changes in mass and stiffness are shown in Table 7. Element 3 clearly shows the lowest standard deviation and hence is the damaged element.

Case 3: Reduced, Noisy Mode Shapes

The final test is the case where the reduced mode shapes are contaminated with noise. For this simulation, 3% (1σ) Gaussian noise is applied to the damaged mode shapes and natural frequencies. The results of this simulation are shown in Table 8.

It is clear from both standard deviations that the third element is the damaged element. Furthermore, the average mass change properly identifies the extent of damage. However, the stiffness damage

Table 8 Damage detection results for reduced, noisy mode shapes

Element	1	2	3	4	5	6
Stiffness standard deviation	0.670	2.763	0.138	1.977	1.045	2.175
Average stiffness change, %	61.50	−124.7	−6.70	179.9	51.2	85.6
Mass standard deviation	0.8415	0.1098	0.0065	0.1196	0.1350	0.0316
Average mass change, %	−11.2	−13.2	−9.59	−0.92	6.92	2.83

is shown to be approximately a 6.7% decrease instead of a 10% decrease. This inaccuracy can be partially explained by the relative insignificance of structural stiffness for the overall stiffness of the blade at high rotation rates. The centrifugal stiffening effect contributes more to the overall blade stiffness than the structural stiffness. Therefore, the mass damage, which decreases the centrifugal forces, is more accurately detected than the structural stiffness damage.

Conclusions

A modal-based damage detection and characterization algorithm is developed for rotating blades in vacuum. The algorithm is an extension to an eigenstructure-assignment-based algorithm that was developed for nonrotating structures. This extension accounts for the large centrifugal forces found in the rotating environment. By including this effect, an enhanced sensitivity to mass damage is obtained at the expense of a reduced sensitivity to structural stiffness change.

The algorithm is validated using analytical data with encouraging results. However, the analytical study demonstrates the need for an improved damage location methodology, which is also developed. Furthermore, the methodology is demonstrated to be effective for both reduced and noisy modes. The extension to eigenstructure assignment for damage detection in rotating structures appears to be a fast and reliable method for use in helicopter main rotor blades. However, experimental validation is required to confirm these analytical results. Sensor implementation and location will play an important part in the viability of this methodology.

Acknowledgments

This work was supported in part by the U.S. Army Research Office under the Smart Structures University Research Initiative, Contract DAAL03-92-G0121, with Gary Anderson serving as Contract Monitor, and in part by the National Rotorcraft Technology Center, Contract NCC2944, with Yung Yu serving as Contract Monitor.

References

[1] Astridge, D. G., "The Health and Usage Monitoring of Helicopter Systems—The Next Generation," *Proceedings of the 41st Forum of the American Helicopter Society*, American Helicopter Society, Alexandria, VA, 1985, pp. 175–188.

[2] Land, J., and Weitzman, C., "How HUMS Systems Have the Potential of Significantly Reducing the Direct Operating Cost for Modern Helicopters Through Monitoring," *Proceedings of the 51st Forum of the American Helicopter Society*, American Helicopter Society, Alexandria, VA, 1995, pp. 744–757.

[3] Cawley, P., and Adams, P. D., "The Location of Defects in Structures from Measurements of Natural Frequencies," *Journal of Strain Analysis*, Vol. 14, No. 2, 1979, pp. 49–57.

[4] Smith, S. W., and Hendricks, S. L., "Damage Detection and Location in Large Space Trusses," *AIAA Structures, Structural Dynamics, and Materials Issues of the International Space Station, A Collection of Technical Papers*, AIAA, Washington, DC, 1988, pp. 56–63.

[5] Zimmerman, D. C., and Kaouk, M., "Structural Damage Detection Using a Subspace Rotation Algorithm," AIAA Paper 92-2521, April 1992.

[6] Lim, T. W., and Kashangaki, T. A. L., "Structural Damage Detection of Space Truss Structures Using Best Achievable Eigenvectors," *AIAA Journal*, Vol. 32, No. 5, 1994, pp. 1049–1057.

[7] Lim, T. W., "Structural Damage Detection Using a Constrained Eigenstructure Assignment," *Journal of Guidance, Control, and Dynamics*, Vol. 18, No. 3, 1995, pp. 411–418.

[8] Doebling, S. W., Farrar, C. R., Prime, M. B., and Shevitz, D. W., "Damage Identification and Health Monitoring of Structural and Mechanical Systems

from Changes in Their Vibration Characteristics: A Literature Review," Los Alamos National Lab., Rept. LA-13070-MS, Los Alamos, NM, Sept. 1995.

[9]Azzam, H., and Andrews, M. J., "The Use of Math-Dynamic Models to Aid the Development of Integrated Health and Usage Monitoring Systems," *Proceedings of the Institution of Mechanical Engineers*, Vol. 206, No. G1, 1992, pp. 71–76.

[10]Ganguli, R., Chopra, I., and Haas, D., "Formulation of a Rotor-System Damage Detection Methodology," *Journal of the American Helicopter Society*, Vol. 41, No. 4, 1996, pp. 302–312.

[11]Ganguli, R., Chopra, I., and Haas, D., "Helicopter Rotor-System Damage Detection Using Neural Networks," *Proceedings of the AIAA 37th Annual Structures, Structural Dynamics, and Materials Conference*, AIAA, Reston, VA, 1996, pp. 645–668.

[12]Lakshmanan, K. A., and Pines, D. J., "Modeling Damage in Composite Rotorcraft Flexbeams Using Wave Mechanics," *Smart Materials and Structures*, Vol. 6, No. 3, 1997, pp. 383–392.

[13]Lakshmanan, K. A., and Pines, D. J., "Detecting Crack Size and Location in Composite Rotorcraft Flexbeams," *Smart Structures and Materials 1995, Smart Structures and Integrated Systems*, Vol. 3041, Society of Photo-Optical Instrumentation Engineers, Bellingham, WA, 1997, pp. 408–416.

[14]Kiddy, J., and Pines, D. J., "Damage Detection of Main Rotor Faults Using a Sensitivity Based Approach," *Smart Structures and Materials 1995, Smart Structures and Integrated Systems*, Vol. 3041, Society of Photo-Optical Instrumentation Engineers, Bellingham, WA, 1997, pp. 611–618.

[15]Johnson, W., *Helicopter Theory*, Dover, New York, 1980, pp. 149–250.

[16]Kiddy, J., and Pines, D., "Constrained Damage Detection Technique for Simultaneously Updating Mass and Stiffness Matrices," *AIAA Journal*, Vol. 36, No. 7, 1998, pp. 1332–1334.

[17]Williams, E. J., and Green, J. S., "A Spatial Curve-Fitting Technique for Estimating Rotational Degrees of Freedom," *Proceedings of the 8th Annual International Modal Analysis Conference*, Society for Experimental Mechanics, Bethel, CT, 1990, pp. 376–381.

A. Berman
Associate Editor